Earth and Planetary Science Letters 371–372 (2013) 49–58

Contents lists available at SciVerse ScienceDirect

Earth and Planetary Science Letters

journal homepage: www.elsevier.com/locate/epsl

Stable isotope evidence for multiple pulses of rapid surface uplift in the Central Andes, Bolivia

Andrew Leier[a,*], Nadine McQuarrie[b], Carmala Garzione[c], John Eiler[d]

[a] Department of Geoscience, University of Calgary, Calgary, AB, Canada T2N 1N4
[b] Department of Geology and Planetary Science, University of Pittsburgh, Pittsburgh, PA 15260, USA
[c] Department of Earth and Environmental Sciences, University of Rochester, Rochester, NY 14627, USA
[d] Division of Geological and Planetary Sciences, California Institute of Technology, Pasadena, CA 91125, USA

ARTICLE INFO

Article history:
Received 7 September 2012
Received in revised form
3 April 2013
Accepted 19 April 2013
Editor: J. Lynch-Stieglitz

Keywords:
oxygen isotope paleoaltimetry
clumped-isotope thermometry
paleoelevation
Andes
orogeny
surface uplift

ABSTRACT

Paleoelevation histories from mountain belts like the Central Andes of Bolivia provide important constraints on the timing and geodynamic mechanisms associated with surface uplift. We present new oxygen and carbon isotope data ($\delta^{18}O$, $\delta^{13}C$, and Δ_{47}) from Oligocene–Miocene strata exposed in the Eastern Cordillera of the Bolivian Central Andes in order to reconstruct both the deformation and paleoelevation history of the region prior to late Miocene time. Paleosol carbonate in strata >24 Ma have $\delta^{18}O_c$ values between −5.7‰ and −9.7‰, and Δ_{47} values indicating paleotemperatures of 32–42 °C. Paleosol carbonate in strata ca. 17 Ma have $\delta^{18}O_c$ values between −11.6‰ and −13.8‰, and Δ_{47} values indicating paleotemperatures of 15–23 °C. These data, interpreted within the context of recent paleoclimate-topography models, suggest Oligocene–early Miocene (29–24 Ma) paleoelevations were between 0 and 1.5 km a.s.l., while middle Miocene (ca. 20–15 Ma) paleoelevations were ~2.5 km a.s.l. Oligocene and Miocene strata are relatively undeformed and overlap folded and faulted Paleozoic rocks in this portion of the Bolivian Eastern Cordillera, indicating much of the change in elevation occurred after upper crustal deformation. Collectively, data from the area record an initial period of upper crustal deformation and exhumation, a subsequent period of sediment deposition and overlap, and then an episode of surface uplift accompanied by negligible upper crustal deformation. The disconnect between the timing of upper crustal deformation and the timing of surface uplift requires geodynamic processes other than upper crustal thickening to explain the Oligocene–Miocene basin and elevation history in the Eastern Cordillera. We propose accommodation for Oligocene–Miocene strata was created in response to the formation and removal of negatively buoyant material in the lowermost crust and mantle lithosphere, and the subsequent increase in surface elevation between ca. 24 and 15 Ma resulted from its removal. Other locations in the Central Andes record similar geological histories over different time periods, suggesting spatial and temporal variation in the removal of lithospheric mantle. Documenting basin extent, age and elevation history provides important constraints on the size and timescale of the geodynamic processes that control surface uplift.

1. Introduction

The elevations of mountain belts reflect multiple geodynamic processes that produce variations in both crustal and mantle lithosphere thicknesses. Surface uplift histories have the potential to provide critical constraints on the processes, forces and feedbacks operating in orogenic systems. Along the western margin of South America, the Andes Mountains reach their greatest height and width in the Central Andes (Fig. 1), where the largest amount of upper crustal shortening has occurred (Kley and Monaldi, 1998; Oncken et al., 2006). Whereas the relationship between the amount of shortening, crustal thickness, and elevation in this region is generally consistent with isostatic expectations (McQuarrie, 2002a), various paleoelevation proxies suggest the timing of upper crustal shortening may have been decoupled from the timing of surface uplift (e.g. Gregory-Wodzicki, 2000; Garzione et al., 2008). Deformation in the Central Andes began by at least 45 Ma, if not earlier (Sempere et al., 1997; DeCelles and Horton, 2003), yet paleoelevation data from the Altiplano of the Central Andes (Fig. 1) suggest the region was at a relatively low elevation (<2 km a.s.l.) until late Miocene time, when it experienced $\sim 2.5 \pm 1$ km of rapid surface uplift between ca. 10 and 6 Ma (Gregory-Wodzicki, 2000; Ghosh et al., 2006; Garzione et al., 2008). These data suggest the timing of upper crustal deformation in the Central Andes may not always be

* Corresponding author. Tel.: +1 403 210 6117.
E-mail address: aleier@ucalgary.ca (A. Leier).

0012-821X/$ - see front matter © 2013 Elsevier B.V. All rights reserved.
http://dx.doi.org/10.1016/j.epsl.2013.04.025

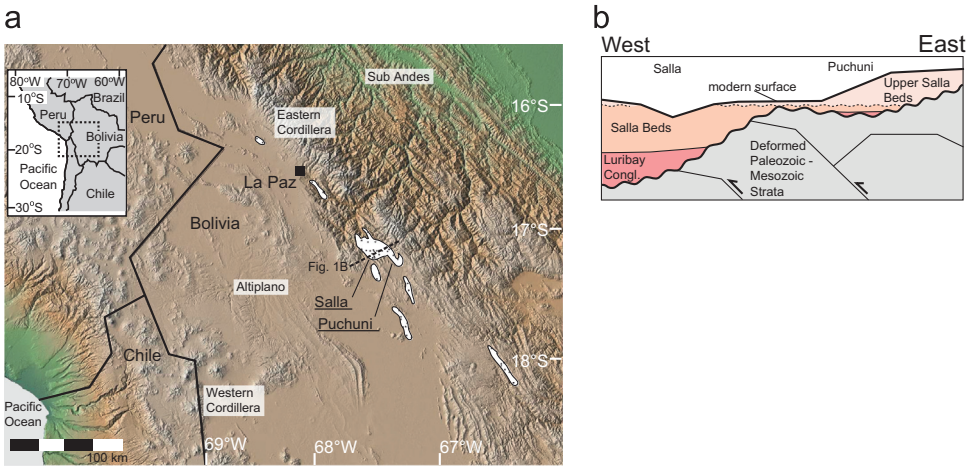

Fig. 1. Location of study area and general tectonostratigraphic relationships. (a) The study area is located along the margin between the Altiplano and Eastern Cordillera south of the city of La Paz, Bolivia. Cenozoic stratigraphic sections are best exposed in Salla and Puchuni. Exposures of Oligocene–Miocene strata are shown in white. (b) Schematic cross-section through the study area showing the flat-lying Oligocene–Miocene strata unconformably overlying highly deformed Paleozoic and minor Mesozoic strata. Samples of paleosol carbonate were collected from the Salla Beds and the Upper Salla Beds. The overlapping and flat-lying nature of the Oligocene–Miocene strata in this area indicates the majority of upper crustal deformation occurred prior to deposition. Luribay Congl.=Luribay Conglomerate.

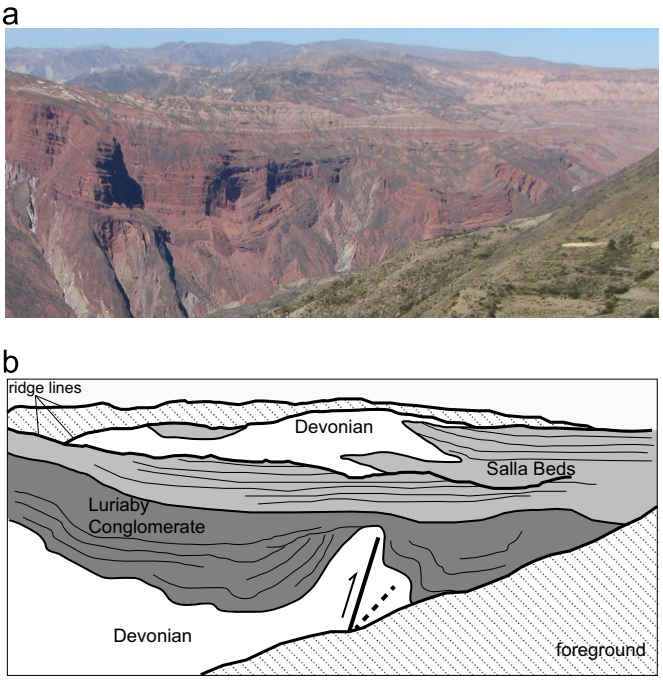

Fig. 2. View looking southeastward (a) and interpretive representation (b) of the Cenozoic strata and underlying Paleozoic units in the Salla area. The folded and faulted Devonian strata (gray in photo, white in representation) in the region are overlain by the Oligocene Luribay Conglomerate (dark red in photo, dark gray in representation) and the Salla Beds (light red to peach in photo, light gray in representation). Beds of the Luribay Conglomerate are folded and displays evidence of growth strata, whereas the overlying Salla Beds are largely undeformed. The Salla Beds onlap and overlap the deformed Devonian strata. Similar stratigraphic relationships are observed elsewhere in the region. These relationships indicate much of the upper crustal deformation in this area preceded deposition of the Salla Beds. (For interpretation of the references to color in this figure legend, the reader is referred to the web version of this article.)

useful for determining the timing of surface uplift. However, other studies indicate the history of upper crustal deformation in the Central Andes is a reliable proxy for surface uplift, and that the elevation of the Central Andes has increased steadily over the past 45 million yr (e.g., Barnes and Ehlers, 2009; Ehlers and Poulsen, 2009; Lamb, 2011; Insel et al., 2012).

The temporal relationship between upper crustal deformation and surface uplift in the Central Andes prior to the late Miocene is poorly constrained, due in large part to the paucity of paleoelevation data from this time period. The oldest direct paleoelevation evidence in the Central Andes comes from marine carbonate of the Upper Cretaceous El Molino Formation (Sempere et al., 1997), which indicates the region was at sea-level at this time. For the time period since the Late Cretaceous, paleoelevation data are sparse and inconsistent. Estimates based on oxygen isotope paleoaltimetry from the Chilean Andes indicate portions of this region were >3.5 km a.s.l. during Eocene time (Quade, J., personal communication). The Central Andes of Bolivia had attained 60–80% of their current crustal thickness by early Miocene time, implying high elevations (McQuarrie, 2002b, 2008b); however, oxygen isotope paleoaltimetry suggests the region was near sea-level (Bershaw et al., 2010). In contrast, estimates from Peru indicate that this portion of the Andes was $\sim$2.5 km a.s.l. by early Miocene time (Picard et al., 2008). Resolving these discrepancies between the magnitude and timing of surface uplift can only be achieved with more extensive paleoelevation data sets.

We present new stable isotope data ($\delta^{18}O$, $\delta^{13}C$, and $T(\Delta_{47})$) from Oligocene–Miocene strata exposed in the Eastern Cordillera of the Bolivian Central Andes (Figs. 1 and 2) in order to provide insight into the earlier paleoelevation history (pre-late Miocene) of this region. These data, integrated with new and existing stratigraphic relationships and structural mapping, provide new constraints on the geologic and geodynamic history of the Eastern Cordillera and the Central Andes.

2. Background

2.1. Tectonic setting and history

The Central Andes are the product of convergence between the oceanic Nazca Plate and the overriding South American Plate. The orogen can be divided from west-to-east into several different tectonogeomorphic zones: the Western Cordillera (magmatic arc); the Altiplano (internally drained plateau); the Eastern Cordillera (folded and faulted Paleozoic strata); and the Subandean Zone (actively deforming Paleozoic–Cenozoic strata; Fig. 1). The location of this study is within the northern Bolivian Eastern Cordillera. Here the Andean fold–thrust belt is characterized by northwest–southeast

trending folds and thrust faults involving Ordovician, Silurian, and Devonian shale and sandstone with lesser amounts of Jurassic sandstone and Cretaceous limestone (Roeder, 1988; Sempere et al., 1990; McQuarrie and DeCelles, 2001). The Eastern Cordillera is split into an east-verging thrust system on the east, and a west-verging portion in the west, the latter of which is referred to as the "Backthrust Belt" (Sempere et al., 1990; McQuarrie and DeCelles, 2001). We examined Cenozoic strata preserved within the west-verging Backthrust Belt of the Eastern Cordillera thrust system (Fig. 1).

Deformation within the Eastern Cordillera in this area commenced by Eocene time (Gillis et al., 2006) and ceased by latest Oligocene time, as inferred from the lower-middle Miocene Salla Beds, which are undeformed and overlie (i.e., overlap) folded and faulted strata in the region (MacFadden et al., 1985; Sempere et al., 1990). The Salla Beds are the source of the stable isotope data ($\delta^{18}O$, $\delta^{13}C$ and $T(\Delta_{47})$) we present in this study.

2.2. Stratigraphy

Oligocene–Miocene strata are preserved in several locations in the Eastern Cordillera over an approximately 200 km by 50 km area (Fig. 1). We examined the Salla Beds in the location of Salla, Bolivia, and the upper continuation of these beds, informally termed the Upper Salla Beds, which are best exposed in the Puchuni region 25 km to the east (Fig. 1). The Salla Beds are an upper Oligocene–lower Miocene, 0.5–1 km thick, flat-lying succession of mudstone with lesser sandstone beds that overlie the Oligocene-age Luribay Conglomerate and deformed Paleozoic strata (Fig. 2) (MacFadden et al., 1985; McRae, 1990; Kay et al., 1998). The Upper Salla Beds in the Puchuni region are a ca. middle Miocene (20–15 Ma), 200 m-thick, flat-lying succession of mudstone and siltstone paleosols that overlie deformed Paleozoic and Mesozoic strata and rare conglomerate (Fig. 2) (Geobol, 1993; Leier et al., 2010). Individual paleosols in the Salla Beds and Upper Salla Beds are typically 1–2 m thick, devoid of sedimentary structures, contain well-developed horizons, and commonly contain pedogenic calcium carbonate nodules (McRae, 1990).

3. Methodology

Carbonate in paleosols from the Salla and Upper Salla Beds was sampled for $\delta^{18}O$ and 'clumped isotope' analyses (Eiler, 2007). Calcium carbonate samples were collected from horizons >50 cm from the paleosurface (typically $\sim$1 m below paleosurface) in both the Salla Beds and Upper Salla Beds. Carbonate nodules themselves were dominantly micritic with rare sparite veins. In the laboratory, the micritic portions of the carbonate nodules were sampled using a micro-drill or dental pick and then ground and homogenized in a mortar. Isotope values were measured from aliquots of the same samples at the University of Rochester and at the California Institute of Technology; full details are located in the Supplementary data section. Oxygen isotope values of carbonate samples ($\delta^{18}O_c$) are reported in the standard notation relative to Vienna Pee-Dee Belemite (VPDB), and calculated water values ($\delta^{18}O_w$, estimated by combining the measured $\delta^{18}O_c$ values and corresponding apparent temperatures of formation based on clumped isotope thermometry) relative to Vienna Standard Mean Ocean Water (VSMOW). Clumped isotope thermometry data are reported as temperatures ($T(\Delta_{47})$) in °C.

3.1. $\delta^{18}O$ and paleoelevation

Oxygen isotope paleoaltimetry is based on the relationship between surface elevation and the $\delta^{18}O_w$ values of meteoric waters (e.g., Poage and Chamberlain, 2001; Rowley and Garzione, 2007). Isotopic values of meteoric water are recorded by precipitating carbonate as a function of temperature (Kim and O'Neil, 1997). Thus, $\delta^{18}O_c$ values of ancient carbonate can be used, with estimates or constraints on paleotemperatures such as $T(\Delta_{47})$ data (see below), to calculate $\delta^{18}O_w$ values. These values can be compared to estimated past $\delta^{18}O$ lapse rates (changes in $\delta^{18}O_w$ with respect to elevation) to reconstruct paleoelevation.

The interpretation of oxygen isotope data in paleoaltimetry studies can be complicated by several factors (e.g., Quade et al., 2007; Ehlers and Poulsen, 2009; Jeffery, 2012). A primary source of uncertainty stems from the fact that paleoelevation estimates typically use modern $\delta^{18}O$ lapse rates. Precipitation in the Central Andes today is dominated by air masses that move from the east to the west. Past variability in factors such as paleoclimate, elevation and pCO_2 values may have had significant effects on the stable isotope values of precipitation and meteoric water in the Central Andes (Ehlers and Poulsen, 2009; Jeffery, 2012). In particular, general circulation models suggest that the creation of topography in the Central Andes has lead to threshold effects in regional climate. Modeling results indicate that as the elevation of the Central Andes reaches 75% of the modern elevation, $\delta^{18}O_w$ values decrease significantly (Ehlers and Poulsen, 2009; Insel et al., 2012). Although there is no specific correction that can be explicitly applied to the measured values, we use these modeling results to address the potential impact of changes in the $\delta^{18}O$ lapse rate in the interpretation of the $\delta^{18}O$ data below.

3.2. Clumped isotope thermometry and paleoelevation

Clumped isotope thermometry $T(\Delta_{47})$ is based on the enrichment, relative to a random isotopic distribution, of the mass 47 isotopologues (mostly ^{13}C–^{18}O–^{16}O) in CO_2 produced by phosphoric acid digestion of carbonate. The analysis, reported as the Δ_{47} value, provides a measure of the proportion of ^{13}C and ^{18}O in a carbonate that are bonded with each other into the same carbonate ion unit. This phenomenon is a function of the temperature at which the carbonate precipitatied or last equilibrated (Eiler, 2007). $T(\Delta_{47})$ values of soil carbonate are thought to record warm-season high temperature values (Breeker et al., 2009; Passey et al., 2010; Quade et al., 2013), although exceptions to this relationship are known in environments having unusual patterns of seasonality in precipitation (Peters et al., 2013). Paleoelevation estimates derived from clumped isotope paleothermometry data are based on the temperature lapse rate, the relationship between temperature and elevation.

Several factors can potentially complicate surface uplift reconstructions employing clumped isotope thermometry; most notably changes in temperature not due to surface uplift (e.g., climate, latitude). Not all cooling recorded in the $T(\Delta_{47})$ data is necessarily due to surface uplift. Models suggest up to several °C of cooling may be related to non-adiabatic mechanisms (Ehlers and Poulsen, 2009), in addition to global or regional climate changes (Poulsen and Jeffery, 2011). We consider these factors in the interpretation of $T(\Delta_{47})$-derived paleoelevation estimates below.

The seasonality of carbonate precipitation is another potential complication in paleoelevation reconstructions based on $T(\Delta_{47})$ values. Soil carbonate typically forms in the warmest months of the year, as the soil dewaters (Breeker et al., 2009; Passey et al., 2010; Quade et al., 2013). This seasonal bias, in combination with incident solar radiation, results in $T(\Delta_{47})$ values near or greater than the warm average monthly temperature (Quade et al., 2013). However, if soil dewatering occurs in non-summer months, the temperature recorded by the soil carbonate may be closer to mean annual temperatures (Peters et al., 2013), which can be

significantly cooler (e.g., < 10 °C) than temperatures of the warmest months (Quade et al., 2013). We assume that the seasonality of precipitation in our study area of the Central Andes did not change significantly between deposition of the Salla Beds and Upper Salla Beds. This supposition is supported by a relatively constant Miocene paleolatitude and paleoclimate modeling results (e.g., Pardo Casas and Molnar, 1987; Insel et al., 2012) that suggest similar paleoprecipitation trends during the Miocene.

3.3. Diagenesis considerations

Stable isotope compositions of ancient carbonate strata can be modified by diagenetic and metamorphic processes; we examined the potential influence of these processes on our results in several ways. Measurements of Cretaceous marine limestones that underlie the Salla and Upper Salla Beds preserve the original stable isotope values (see Results). Thus, there is little reason to believe the more shallowly buried strata we examined in this study are pervasively modified (e.g., Leier et al., 2009). Nevertheless, differences in petrography, chemistry, and fluid flow-history may have permitted alteration of shallow paleosols. Therefore, we also made petrographic observations of thin sections from several of the studied carbonate nodules and noted that they are dominated by micritic textures—generally an indication that these nodules have experienced little-to-no recrystallization (Garzione et al., 2004; Leier et al., 2009). Only micritic portions of the carbonate nodules were sampled for isotopic analysis.

The samples examined are part of a sedimentary section believed to have never been buried to depths great than 1 km (Geobol, 1993; Quade et al., 2007). This is significant because thermal resetting of the carbonate clumped isotope thermometer (from lattice-scale redistribution of isotopes) in calcite appears to be detectable only with prolonged heating to ~100 °C or more, and substantial only when heating exceeds ~150 °C (Eiler, 2007, 2011; Passey and Henkes, 2012; Quade et al., 2013). Our samples were likely never heated to temperatures in excess of 60 °C (assuming a typical geothermal gradient) and thus should only have undergone diagenetic resetting if they were subjected to dissolution/reprecipitation or other replacement or recrystallization. These processes leave visible petrographic evidence that we did not observe.

4. Results

4.1. $\delta^{18}O_c$ values

Carbonate from the Salla Beds have $\delta^{18}O_c$ values between −5.7‰ and −9.7‰, with the majority between −6‰ and −8‰ (Fig. 3 and Table 1). Carbonate from the Upper Salla Beds have $\delta^{18}O_c$ values between −11.6‰ and −13.8‰, with the majority having values of approximately −12‰ (Fig. 3). Underlying Cretaceous marine limestones sampled in the area have $\delta^{18}O_c$ values of −1.3‰ (Table 1), which is consistent with expected marine values and suggests minimal diagenetic alteration of $\delta^{18}O_c$ values in this area.

4.2. $T(\Delta_{47})$ values

The $T(\Delta_{47})$ values from the Salla Beds and the Upper Salla Beds differ (Fig. 3). Carbonate from the Salla Beds have $T(\Delta_{47})$ values of 32–42 °C, whereas carbonate from the Upper Salla Beds have Δ_{47} values recording temperatures of 15–23 °C (Fig. 3). Temperatures recorded in the Salla Beds are consistent with those from other low-latitude, warm climates (Quade et al., 2007, 2013; Passey et al., 2010).

5. Paleoelevation estimates

5.1. Isotope data

Paleoelevation can be estimated using the $T(\Delta_{47})$ values and $\delta^{18}O_c$ values of each sample, calculating the paleometeoric $\delta^{18}O_w$ values, and then estimating paleoelevation using the modern thermal and $\delta^{18}O$ lapse rates in the Central Andes. For the Salla Beds, the average $T(\Delta_{47})$ value of 36 ± 4 °C, yields $\delta^{18}O_w$ values that range between −3.5‰ and −4.8‰ and average −4.0‰. Using the modern relationship (from Bershaw et al., 2010) between oxygen isotopes in meteoric water and elevation in the Central Andes ($y = -536.4x - 3202$; where y = elevation in meters, and $x = \delta^{18}O_w$ in ‰) results in a paleoelevation estimate of -1.1 km $\pm$ 0.5 km for the Salla Beds. A paleoelevation estimate of ~1 km below sea-level is obviously implausibly low. The lower limit of paleoelevation during deposition of the Salla Beds is interpreted to be 0 m a.s.l.,

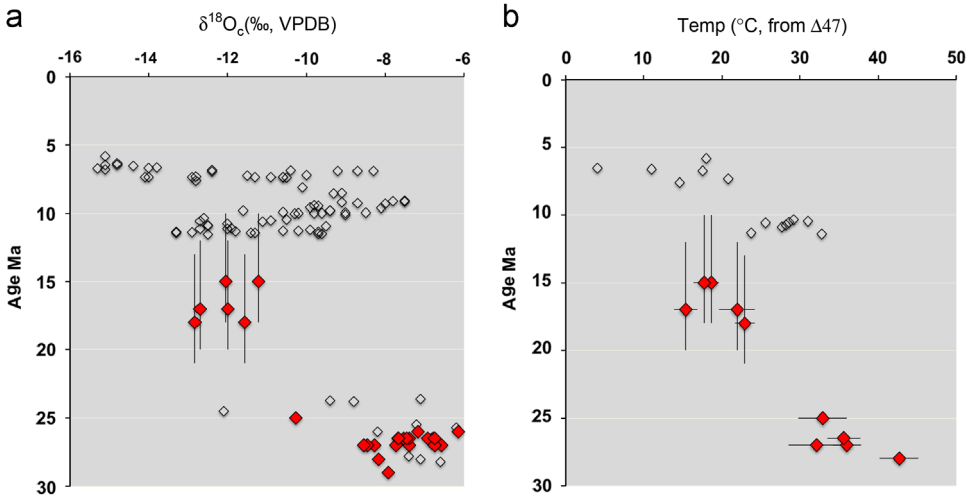

Fig. 3. Results from isotopic analyses of paleosol carbonate from the Salla and Upper Salla Beds in the study area. New results are designated by the infilled diamonds; unfilled diamonds are published data from samples in the Central Andes (Garzione et al., 2008). See Table 1 for actual values. (a) Oxygen-isotope values ($\delta^{18}O_c$, in ‰) of paleosol carbonate from the Salla (29–24 Ma) and Upper Salla Beds (ca. 17 Ma). Oxygen-isotope values are more negative in the younger Upper Salla Beds. (b) Temperatures (in °C) of precipitation of paleosol carbonate from the Salla and Upper Salla Beds based on $T(\Delta_{47})$ values. Temperatures associated with the Upper Salla Beds are less than those associated with the Salla Beds. See Supplementary data for full results.

Table 1
References: Dennis et al. (2011) and Huntington et al. (2009).

Summary table														
Sample	Lat.	Long.	Elev (m)	δ18O*[a]	δ13C*[a]	δ18O*[b]	δ13C*[b]	Δ47 CIT[d]	Δ47[e]	Δ47 Temperature (°C)	Δ47 T replicate 1	Δ47 T replicate 2[c]	Δ47 Average T (°C)	Δ47 St. dev.
Salla Beds														
AL 1-118	−17.150	−67.629	3725			−9.66	−5.75	0.547	0.622	44.43	40.90		42.66	2.49
AL 1-128	−17.150	−67.629	3733	−7.9	−5.4	−8.59	−5.22	0.600	0.649	37.33	36.75	33.89	35.98	1.83
AL 1-131	−17.150	−67.629	3733	−8.6	−5.6	−8.60	−5.32	0.615	0.665	29.56	34.66		32.10	3.60
AL 2-36c	−17.177	−67.619	3797	−7.0	−6.7									
AL 2-36m	−17.177	−67.619	3797	−7.7	−6.7									
AL 2-36m2	−17.177	−67.619	3797	−7.3	−6.6									
AL 2-44	−17.177	−67.620	3812	−7.6	−6.9	−7.98	−6.56	0.601	0.650	34.15	37.05		35.59	2.05
AL 3-41	−17.207	−67.635	4051		−7.8	−7.68	−7.99	0.612	0.662	35.09	30.69		32.88	3.11
3	−17.164	−67.618	3825	−6.6	−5.3									
4a	−17.159	−67.628	3749	−8.9	−5.4									
4b	−17.159	−67.628	3749	−8.8	−5.3									
4c	−17.159	−67.628	3749	−6.8	−4.8									
6	−17.158	−67.628	3737	−8.7	−5.4									
7a	−17.163	−67.628	3720	−7.0	−5.4									
8a	−17.167	−67.627	3700	−7.8	−5.9									
8b	−17.167	−67.627	3700	−8.2	−5.8									
9a	−17.169	−67.624	3748	−6.9	−5.3									
26	−17.206	−67.622	4103	−6.4	−6.9									
43	−17.181	−67.587	4071	−6.4	−6.8									
sl1-56	−17.153	−67.624	3687	−8.2	−6.0									
sl1-142	−17.156	−67.626	3703	−6.0	−5.6									
sl1-163	−17.157	−67.626	3710	−8.5	−5.6									
Upper Salla Beds														
AL 6-46	−17.240	−67.462	4161			−13.28	−5.62	0.655	0.707	24.22	22.99	21.60	22.93	1.30
AL 6-49	−17.240	−67.462	4155	−13.2	−5.7									
36a	−17.233	−67.467	4149	−13.1	−7.4	−13.85	−7.47	0.691	0.744	14.27	16.43		15.34	1.52
36b	−17.233	−67.467	4149	−12.4	−7.8	−13.17	−7.61	0.660	0.711	20.33	23.56		21.94	2.28
37a	−17.224	−67.471	4122	−12.8	−6.4	−12.86	−6.12	0.675	0.727	17.97	19.31		18.63	0.94
37b	−17.224	−67.471	4122			−12.95	−4.93	0.680	0.732	16.73	18.75		17.73	1.42
El Molino Formation (*Cretaceous marine*)														
53	−17.238	−67.352	4084	−1.3	−0.8									

See Supplementary data for complete results and detailed methodology.

* in ‰ (VDPB).
[a] Measurements made at the University of Rochester SIREAL Lab.
[b] Measurements made at Cal Tech.
[c] Δ47 T replicate 2 was from 2009 session; all other Δ47 T data from 2010 session.
[d] Reference frame of Huntington et al. (2009).
[e] Approximate conversion to reference frame of Dennis et al. (2011).

based on the fact that the Salla Beds are nonmarine deposits (MacFadden et al., 1985; McRae, 1990). Our results are consistent with those of Bershaw et al. (2010), who examined fossil teeth from the Salla Beds. Several factors discussed in detail by these authors likely contribute to the negative elevation estimates for the Salla Beds, including the application of a modern $\delta^{18}O$ lapse rate to an ancient setting, a more arid climate in western South America as suggested by climate modeling (Ehlers and Poulsen, 2009), or a smaller continental effect and/or a larger vapor source from the more proximal Pacific ocean.

The upper limit of paleoelevation during deposition of the Salla Beds is more difficult to determine, but recent models provide constraints (Fig. 4). Isotope-tracking climate models predict $\delta^{18}O_w$ values within the Central Andes for various paleoelevation scenarios (Insel et al., 2012), which can then be compared to the $\delta^{18}O_w$ values we have reconstructed from the Salla Beds. The $\delta^{18}O_w$ values calculated from the Salla Beds fall within a permissible range of 0 to approximately 1 km a.s.l. based on the models (Fig. 4). The modeling results of Insel et al. (2012) reflect a late Miocene climate, which was likely cooler than that of the late Oligocene–early Miocene (e.g., Zachos et al., 2001). Warmer temperatures would reduce the $\delta^{18}O$ lapse rate and have the effect of shifting the envelope in Fig. 4 to more positive $\delta^{18}O_w$ values, which could lead to underestimates of paleoelevation by 14% and $>40\%$ in climates with 2 and 4 times the preindustrial pCO_2 levels, respectively (e.g., Poulsen and Jeffery, 2011). The result is that the modeled range of $\delta^{18}O_w$ values would allow for an upper paleoelevation limit as high as approximately 1.5 km a.s.l. for the Salla Beds. Paleoelevation estimates of 0–1.5 km a.s.l. for the Salla Beds are supported by age-equivalent samples from low elevation regions. Oxygen isotope values of late Oligocene fossil teeth from areas <1 km a.s.l near coastal Brazil yield $\delta^{18}O_w$ values of −2.7‰ and −3.0‰ (Bershaw et al., 2010), similar to the −4‰ $\delta^{18}O_w$ values from the Salla Beds. Moreover, the $T(\Delta_{47})$ results from the Salla Beds are consistent with relatively low paleoelevations, with values similar to those from low elevations in modern Bolivia (http://www.climate-zone.com, 2012)

Upper Salla Beds have an average $T(\Delta_{47})$ value of 20 ± 3 °C, yielding $\delta^{18}O_w$ values that range between −11.3‰ and −13.5‰ and average −12.0‰ (Fig. 3). Employing the modern $\delta^{18}O_w$–elevation lapse rate in the Central Andes yields a paleoelevation estimate of 3.2 ± 0.5 km. To test this estimate, we compare these results with those from Insel et al. (2012). If all of the $\delta^{18}O_w$ values from the Upper Salla Beds are included and compared to the modeling results, paleoelevation during deposition of the Upper Salla Beds is approximately 3 km or greater (Fig. 4). If the most negative $\delta^{18}O_w$

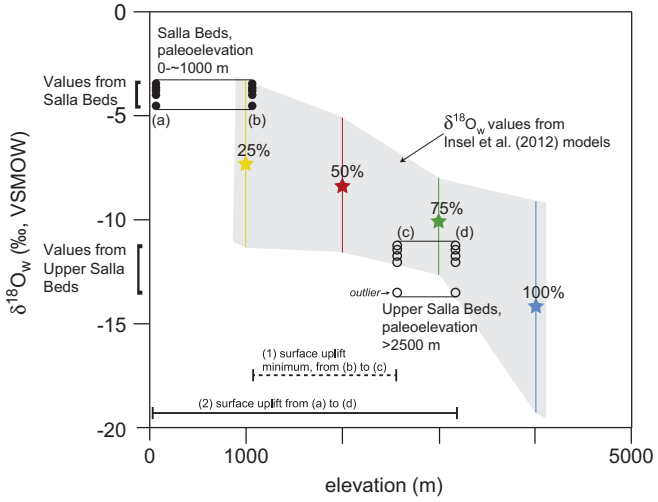

Fig. 4. Calculated paleometeoric water values ($\delta^{18}O_w$) from the Salla and Upper Salla Beds (closed and open circles, respectively) plotted on a $\delta^{18}O_w$–elevation relationship (y and x axes, respectively) from modeling results of Insel et al. (2012). The stars represent an average $\delta^{18}O_w$ value for the late Miocene Central Andes at 25%, 50%, 75%, and 100% of modern Andean elevations. The gray area is the envelope of 2σ variation. The $\delta^{18}O_w$ values from the Salla Beds are shown along the y-axis (approximately −4‰). These values correspond to modeled $\delta^{18}O_w$ values between a minimum elevation of 0 km a.s.l., shown by (a) to a maximum elevation of ~1 km a.s.l., shown by (b). The models of Insel et al. (2012) suggest it is unlikely $\delta^{18}O_w$ values like those calculated from the Salla Beds would be present at paleoelevations greater than ~1 km. Thus, the paleometeoric water values from the Salla Beds are consistent with paleoelevations of approximately 0–1 km a.s.l. Warmer temperatures during the early Miocene would have the effect of shifting the averages and 2σ envelope to less negative $\delta^{18}O_w$ values, permitting the Salla Bed data to have been possible at elevations as high as ~1.5 km a.s.l. The $\delta^{18}O_w$ values calculated from the Upper Salla Beds are shown along the y-axis (approximately −12‰). (c) Displays the minimum paleoelevation if the most negative $\delta^{18}O_w$ outlier is omitted, and (d) displays the minimum paleoelevation if the most negative $\delta^{18}O_w$ outlier is included. These comparisons suggest the Upper Salla Beds were deposited at elevations of at least 2.5 km a.s.l. The lines at the base of Figs. 1 and 2, display the minimum amount of surface uplift between deposition of the Salla Beds and the Upper Salla Beds: (approximately 1.5 km, from (b) of the Salla Beds to (c) of the Upper Salla Beds), and (2) the maximum amount of surface uplift (approximately 3 km) within the constraints of the modeling results. Based on additional data, the minimum amount is considered more likely. See text for further discussion. For a complete explanation of the modeling results see Insel et al. (2012).

value is omitted ("outlier" in Fig. 4), the $\delta^{18}O_w$ values indicate paleoelevations of approximately 2.5 km or greater (Fig. 4). Once again, warmer temperatures would shift the envelope to more positive $\delta^{18}O_w$ values, which would slightly increase paleoelevation estimates.

An alternative method for estimating elevation gain between the Salla Beds and Upper Salla Beds utilizes the temperature difference of 16 °C recorded in $T(\Delta_{47})$ data from paleosols from both stratigraphic successions. Using the modern temperature lapse rate of 5 °C/km for the Central Andes (Gonfiantini et al., 2001), the temperature difference of 16 °C requires an increase in surface elevation of 3.3 km. However, not all cooling is necessarily due to surface uplift, as models suggest up to 6.5 °C of cooling may have been related to non-adiabatic mechanisms (Ehlers and Poulsen, 2009). If 6.5 °C of the 16 °C difference is attributed to non-adiabatic cooling, the magnitude of surface uplift is reduced to approximately 2 km.

Estimates of late Miocene surface uplift can be used as an additional constraint on the paleoelevation history of the Central Andes during ca. middle Miocene time. The cumulative amount of surface uplift in this portion of the Central Andes should equal the current elevation, which is approximately 4 km a.s.l. (see Table 1 for sample elevations). Paleoelevation studies suggest ~2.5 ± 1 km of

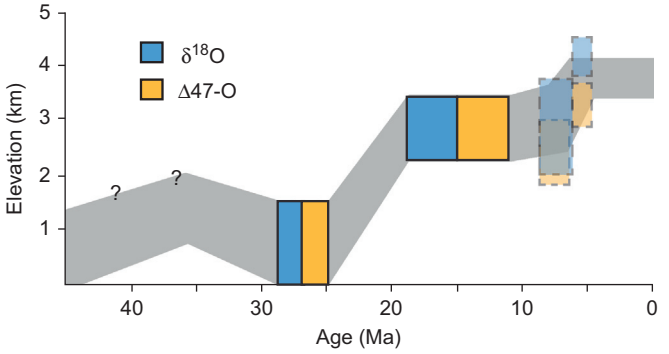

Fig. 5. Reconstructed paleoelevation history of the Eastern Cordillera in the northern Central Andes of Bolivia. New constraints from this study are depicted in solid colors ($\delta^{18}O$—oxygen isotope data; Δ47-O—clumped isotope data), transparent colors constraining the late Miocene history are from published results from the Altiplano (Garzione et al., 2008). The paleoelevation history prior to the late Oligocene (50–30 Ma) is poorly constrained, but here is suggested using shortening estimates and isostatic compensation (e.g., McQuarrie, 2002b). Between 29 and 24 Ma, during deposition of the Salla Beds, the elevation in the study area was between approximately 0 and 1.5 km a.s.l. By ca. 17 Ma (age estimates depicted in the figure include uncertainty), during deposition of the Upper Salla Beds, the elevation was approximately 2.5 km a.s.l. Surface uplift during the late Miocene elevated the region from ~2.5 km a.s.l. to the current ~4 km a.s.l. The inability to quantify soil temperature lapse rates at the time of soil carbonate formation requires a cautious view of these paleoelevation estimates. However, we provide independent paleoelevation estimates from the $T(\Delta_{47})$ results for comparison to the results from oxygen isotopes and note that both methods are in general agreement that ~2 km or more surface uplift occurred during Miocene time. (For interpretation of the references to color in this figure legend, the reader is referred to the web version of this article.)

surface uplift occurred in the adjacent Altiplano of the Central Andes from late Miocene-present (Gregory-Wodzicki, 2000; Garzione et al., 2008). To attain the current 4 km elevation, these late Miocene paleoelevation studies imply the paleoelevation prior to late Miocene time was approximately 0.5–2.5 km a.s.l. Notably, a paleoelevation estimate of ~3 km from the Upper Salla Beds (see above) would overpredict modern elevations by 0.5–1.5 km if combined with 2.5 ± 1 km of late Miocene surface uplift. Thus, the lower estimates of paleoelevation (~2.5 km) derived from the Upper Salla Beds, as well as the lower limit of late Miocene elevation change (~1.5 km) are considered more plausible.

In summary, isotope-derived paleoelevation values, modified and constrained with climate modeling (e.g., Poulsen and Jeffery, 2011; Insel et al., 2012) suggests an elevation change from 0–1.5 km a.s.l. (Salla Beds) to ~2.5 km a.s.l. (Upper Salla Beds) in the ca. middle Miocene, which was later followed by surface uplift from ~2.5 km a.s.l. to 4 km a.s.l. during the late Miocene (Fig. 5).

5.2. Corroborative evidence of surface uplift

Geological evidence from the lower Miocene stratigraphic record in the adjacent Altiplano supports the stable isotope evidence of surface uplift in the Eastern Cordillera during ca. middle Miocene time. Provenance data from the Altiplano indicate that sediment deposited in the Altiplano prior to early Miocene time was derived from the Western Cordillera and transported eastward (Horton et al., 2001). However, by early Miocene time, significant volumes of sediment were being derived from the Eastern Cordillera and transported westward, into the Altiplano (Fig. 6; Horton et al., 2001). This change in sediment provenance indicates surface uplift in the Eastern Cordillera relative to the Altiplano (Fig. 6) and is consistent with the change in $\delta^{18}O_c$ values (Fig. 3) and inferred paleoelevation history of the Eastern Cordillera (Fig. 5).

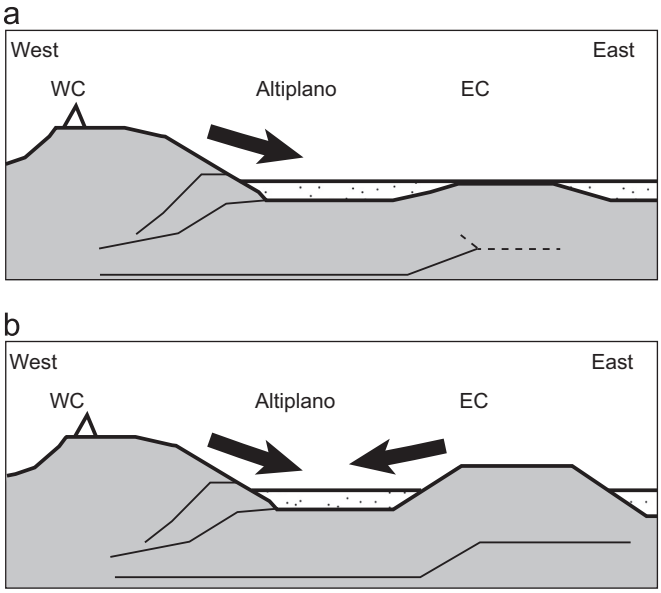

Fig. 6. Provenance data from the adjacent Altiplano support the stable isotope data indicating surface uplift in the Eastern Cordillera. (a) Prior to early Miocene time, sediment in the Altiplano of the Central Andes was derived from the west. (b) During early Miocene time, sediment was shed from the Eastern Cordillera into the Altiplano, indicating surface uplift in the Eastern Cordillera relative to the Altiplano. The primary area of surface uplift is inferred to be the Eastern Cordillera. Provenance data and reconstruction from Horton et al. (2001). WC=Western Cordillera, EC=Eastern Cordillera.

6. Discussion

6.1. Geologic context and geodynamic mechanisms

The combination of exhumation records, depositional histories, and paleoelevation data provide important constraints on the geologic history of this portion of the Eastern Cordillera. Between ca. 50 and 30 Ma, immediately prior to deposition of the Oligocene–Miocene Salla Beds, the Backthrust Belt of the Eastern Cordillera accommodated ~170 km of shortening, which was accompanied by 4–7 km of exhumation (Gillis et al., 2006; McQuarrie et al., 2008a). In our specific study area, the level of exposure in the deformed Paleozoic section (Devonian and upper Silurian units) underlying the Salla and Upper Salla Beds suggests 4.5–6 km of material was removed prior to deposition (Fig. 2). Estimated erosion rates (0.2–0.3 mm/yr) are consistent with ~1.5 km of relief (Montgomery and Brandon, 2002) between the Eastern Cordillera and surrounding regions from ca. 50 to 30 Ma (Fig. 5).

Deposition of the Salla Beds occurred as upper crustal deformation in this area ceased (Fig. 2; Sempere et al., 1990; McQuarrie, 2002b). The paleoelevation data presented here indicate the Salla Beds were deposited on top of deformed Paleozoic units at relatively low elevations (≤1.5 km a.s.l.) despite the fact that crustal thicknesses are estimated to have been ~45–60 km at this time (McQuarrie, 2002b). Following deposition of the Salla Beds and prior to or coincident with deposition of the Upper Salla Beds, surface uplift occurred. The increase in surface elevation did not involve upper crustal deformation in this area as the Salla Beds are relatively flat-lying and undeformed today (Sempere et al., 1990; McQuarrie, 2002b). Therefore, any geodynamic mechanism explaining the Oligocene–Miocene evolution of this portion of the Eastern Cordillera must be able to account for the following: basin formation and sediment overlap in the Eastern Cordillera following millions of years of upper crustal deformation and exhumation; paleoelevations lower than what would be estimated (isostatically) following upper crustal shortening and thickening; and subsequent surface uplift that did not involve upper crustal deformation.

The transition from millions of years of exhumation to several millions of years of deposition in the northern Eastern Cordillera is rather atypical. The Salla Beds overlie highly folded and faulted Paleozoic strata over a region that extends ~200 km north-to-south along the Eastern Cordillera (Fig. 1). Due to post-depositional erosion, the original east–west dimension of this depocenter cannot be determined, but was likely larger than the ~50 km width that is preserved today. A possible mechanism to explain the change from exhumation to deposition is the damming of a river through the blockage of a drainage outlet. Surface uplift associated with a nearby thrust fault could have blocked a drainage outlet, effectively raising local base-level, and initiating deposition (e.g. Burbank et al., 1996; Sobel et al., 2003). Although this scenario would be possible in an area where extensive and continuous structures are larger than the damned drainage area, it is unlikely this scenario could have caused the Oligocene–Miocene deposition in the region. The north–south extent of the deposits (~200 km) is far greater than the along-strike continuity of any thrust fault or fold in this area, which are limited to ~ < 50 km along strike (McQuarrie and DeCelles, 2001). Moreover, this mechanism does not adequately explain the extent of sedimentation in the region, where paleotopographic features are buried by Oligocene–Miocene strata (MacFadden et al., 1985; McRae, 1990; Geobol, 1993; Leier et al., 2010), nor the pronounced negative shift in oxygen isotope values and temperatures between the Salla and Upper Salla Beds. Surface uplift resulting from lower crustal flow (e.g., Clark and Royden, 2000; Lamb, 2011) is also considered unlikely because at the time of surface uplift, the Eastern Cordillera would have been the location of the thickest crust, implying that the flow of material would have been away from the Eastern Cordillera and not towards it. In addition, lower crustal flow as a thickening mechanism does not explain the formation of the 200 by 50^{+} km Salla basin.

Geophysical and geochemical data indicate lowermost crust and mantle lithosphere have been removed from beneath the Central Andes as the crust has been shortened (e.g., Kay and Kay, 1993; Hoke et al., 1994; Lamb and Hoke, 1997; Beck and Zandt, 2002). We propose that upper crustal shortening and thickening, coupled with the accumulation and subsequent removal of negatively buoyant material in the lowermost crust and mantle lithosphere, were responsible for the Oligocene–early Miocene geologic history of this portion of the Eastern Cordillera (Fig. 7). Upper crustal shortening and thickening in the Eastern Cordillera from ca. 50 to 30 Ma is postulated to have been accommodated at depth by the development of a metastable package of eclogitic material in the lowermost crust and thickening of the underlying mantle lithosphere (e.g. McQuarrie et al., 2005; Sobolev and Babeyko, 2005; DeCelles et al., 2009). The accumulation of this material and downwelling associated with its initial removal can account for the low paleoelevations in this area, despite the thickened crust, during late Oligocene–earliest Miocene time (Fig. 7). In addition, this mechanism can produce surficial downwarping (e.g. Saleeby and Foster, 2004), providing accommodation for deposition of the Salla Beds and explaining the overlapping relationship of this unit to the underlying deformed Paleozoic strata (Sempere et al., 1990; McQuarrie and DeCelles, 2001). Following the removal of the negatively buoyant material, the replacement of mantle lithosphere with less dense asthenosphere would result in a subsequent isostatic rise of the surface (e.g. Garzione et al., 2006; Gogus and Pysklywec, 2008; Hoke and Garzione, 2008). This mechanism can explain the increase in surface elevation and the undeformed nature of the Salla Beds.

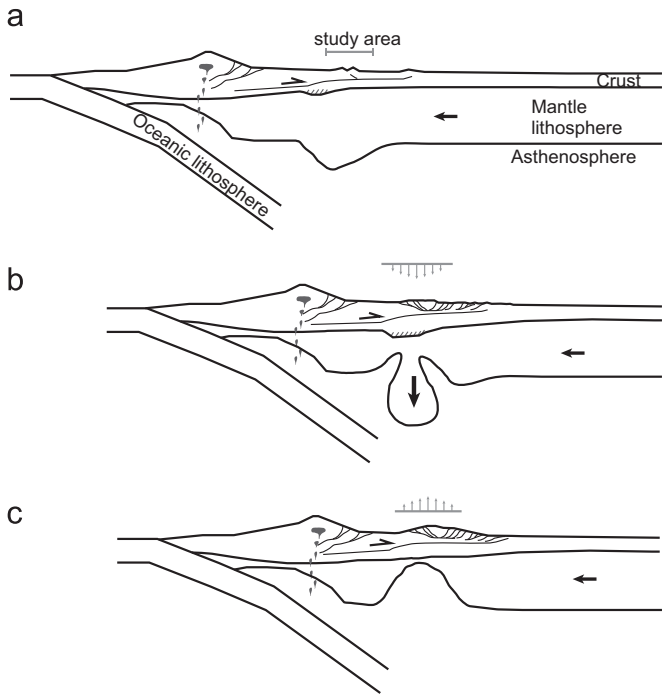

Fig. 7. Schematic diagram of the proposed Oligocene–Miocene geodynamic evolution of the Central Andes in northern Bolivia; profile-view, looking ~north. (a) Along the western margin of central South America shortening and thickening in the crust between ca. 50 and 30 Ma is accommodated at depth by the accumulation of excess mantle lithosphere. In addition, the thickening of the crust may have led to the formation of an eclogitic root in the lowermost crust (hatchered area). (b) The accumulation and removal of this material results in a downwarping of the overlying crust. This mechanism explains how accommodation was created atop deformed and thickened crust, allowing the overlapping deposition of the late Oligocene and early Miocene Salla Beds (see also Fig. 2). This mechanism also explains why relatively low paleoelevation values are recorded for this region despite crustal thicknesses estimated to be approximately 50 km. (c) Following deposition of the Salla Beds (29–24 Ma) and prior to or coincident with deposition of the Upper Salla Beds (ca. 17 Ma), the removal of the excess material and the isostatic rebound results in surface uplift in the overlying portion of the orogen. This mechanism explains the change in oxygen isotope values (see Figs. 3 and 4) and how the Salla Beds remain relatively flat-lying and undeformed (see Fig. 2). The surface uplift during this period is recorded by the change in sediment provenance in the adjacent Altiplano (see Fig. 6).

6.2. Localized deposition associated with regions of lithospheric removal

Cenozoic strata in the area of the Eastern Cordillera examined in this study record the waning stages of upper crustal deformation, the formation of a sub-regional basin and the sediment overlap of paleotopography, and a subsequent episode of surface uplift. Similar histories are present in several other locations in the hinterland of the Central Andes. In the Corque-Corocoro area of the Altiplano, increased sedimentation rates between ca. 13 and 10 Ma resulted in the accumulation of approximately 4 km of sediment in a 100 km wide by 200 km long depression (Garzione et al., 2008; Lamb, 2011). Immediately following deposition, between ca. 10 and 6 Ma, the region experienced an episode of surface uplift (~2.5 ± 1 km) that resulted from partial removal of dense lower lithosphere from beneath the area (Garzione et al., 2006). Similarly, in the southern portion of the Altiplano, a basin formed between 20 and 16 Ma, as upper crustal deformation in the region waned (Horton, 1998). $T(\Delta_{47})$ data indicate a period of rapid surface uplift of ~1.5 km occurred between 16 and 13 Ma (Garzione et al., in review) as the region transitioned from a depocenter to an area of non-deposition. Linking episodes of surface uplift to the spatial extent of basins that precede/accompany them (e.g., Saleeby and Foster, 2004) may provide critical constraints on the length-scales and geodynamics of mantle-driven surface uplift.

6.3. Steady versus unsteady surface uplift

Recent debate has centered on whether the current elevation of the Central Andes has been attained by steady surface uplift (e.g., Barnes and Ehlers, 2009) or primarily during geologically brief periods of rapid surface uplift (e.g., Gregory-Wodzicki, 2000; Garzione et al., 2008). Our data, when combined with existing stable isotope data from the Central Andes suggests an elevation change from 0–1.5 km a.s.l. to ~2.5 km a.s.l. in the ca. middle Miocene followed by later surface uplift from ~2.5 km a.s.l. to 4 km a.s.l. during the late Miocene (Fig. 5). These data ostensibly support a more punctuated history of surface uplift in the Central Andes (Fig. 5); however, they may also accommodate a more steady surface uplift history. Inherent uncertainty in absolute paleoelevation data (e.g., Rowley and Garzione, 2007), mean that the range of permissible paleoelevations through time is considerable (e.g., Barnes and Ehlers, 2009; Ehlers and Poulsen, 2009; Insel et al., 2012). Moreover, the relative scarcity of paleoelevation proxies in the geologic record means we currently cannot reconstruct a continuous record for the past 45 million yr (e.g., Fig. 5), which may also give rise to a more punctuated-appearing paleoelevation history. However, even with these considerations, there remain inconsistencies between paleoelevations and crustal shortening histories. Incorporating the full range of permissible paleoelevation values suggested by paleoclimate modeling, oxygen isotope-derived paleoelevations during the early Miocene (0–1.5 km a.s.l.) are at a minimum 1 km lower than elevations predicted by shortening estimates (McQuarrie, 2002b) and isostatic compensation (predicting ~2.5 km a.s.l.). This disparity requires some component of negative buoyancy. The 2.5–3.0 km elevation reconstructed from the Upper Salla Beds in ca. middle Miocene time suggests the removal of the negatively buoyant component. Thus, while the exact magnitude of surface uplift remains uncertain, we propose that the combined deformation, basin, and stable isotope data argue for modest (e.g., 0.5 km) to moderate (1.5 km) punctuated surface uplift in the Miocene, where surface uplift did not coincide with the steady upper crustal deformation that preceded both basin formation and the subsequent increase in elevation (e.g., Fig. 7).

7. Conclusions

Well-constrained paleoelevation histories from mountain belts are critical for understanding the geodynamic processes that drive changes in surface elevation. This study presents new stable isotope data ($\delta^{18}O$, $\delta^{13}C$, and $T(\Delta_{47})$) from Oligocene–Miocene strata exposed in the Eastern Cordillera of the Bolivian Central Andes, expanding the temporal record of paleoelevation proxies. Paleosol carbonate in strata >24 Ma have $\delta^{18}O_c$ values between −5.7‰ and −9.7‰, and $T(\Delta_{47})$ values indicating paleotemperatures of 32–42 °C. Paleosol carbonate in strata ca. 17 Ma have $\delta^{18}O_c$ values between −11.6‰ and −13.8‰, and $T(\Delta_{47})$ values indicating paleotemperatures of 15–23 °C. Although determining paleoelevation from these data is complicated by past climatic and climate-topographic variables, the combination of geological data and recent climate modeling results provides a means for constraining likely values. Using these constraints, we interpret the paleoelevation in the area during Oligocene–early Miocene time was between 0 and 1.5 km a.s.l. Paleoelevation in the area during ca. middle Miocene time is interpreted to have been ~2.5 km a.s.l. Thus, isotope-based paleoelevation values, modified and constrained with climate modeling, suggests an elevation change from 0–1.5 km a.s.l. to ~2.5 km a.s.l. in ca. middle Miocene time

followed by later surface uplift from ~2.5 km a.s.l. to 4 km a.s.l. during the late Miocene (Fig. 5).

Upper crustal deformation and the surface uplift history in this portion of the Eastern Cordillera are decoupled. Oligocene and Miocene strata are relatively undeformed and overlap folded and faulted Paleozoic rocks in this portion of the Bolivian Eastern Cordillera, indicating much of the surface uplift occurred after deformation. Geologic data from the area record an initial period of upper crustal deformation and exhumation, a subsequent period of sediment deposition and overlap, and then an episode of surface uplift not accompanied by upper crustal deformation. Abrupt changes in $\delta^{18}O$ and $T(\Delta_{47})$ values derived from paleosol carbonate nodules across the Central Andes are best explained by regionally-variable, and diachronous episodes of surface uplift. We suggest that the dimensions of the basins that record low elevation isotopic signatures help constrain the spatial scale of the downwelling lithosphere, while the shift in isotopes preserved in the youngest sediments record the replacement of mantle lithosphere with less dense asthenosphere and subsequent isostatic rise in surface elevation.

Acknowledgments

Funding for this work has been provided by the National Science Foundation – Division of Earth Sciences, and the Natural Sciences and Engineering Research Council of Canada. We would like to thank P. Higgins and N. Kitchen, and M. Cosca. We would also like to thank S. Long, T. Cecil-Cockwell, and T. Dixon. Additional assistance was provided by S. Tawackoli, and C. Ossio. We thank B. McFadden for his guidance. Discussions with C. Poulson and J. Barnes and many others helped focus the manuscript. We thank three anonymous reviewers who edited a previous version. The manuscript was greatly improved by the comments and careful edits of two anonymous reviewers. We also thank editor J. Lynch-Stieglitz.

Appendix A. Supplementary materials

Supplementary data associated with this article can be found in the online version at http://dx.doi.org/10.1016/j.epsl.2013.04.025.

References

Barnes, J.B., Ehlers, T.A., 2009. End member models for Andean Plateau uplift. Earth-Sci. Rev. 97, 105–132.
Beck, S., Zandt, G., 2002. The nature of orogenic crust in the central Andes. J. Geophys. Res. 107, 2230.
Bershaw, J., Garzione, C.N., Higgins, P., MacFadden, B.J., Anaya, F., Alvarenga, H., 2010. Spatial-temporal changes in Andean plateau climate and elevation from stable isotopes of mammal teeth. Earth Planet. Sci. Lett. 289, 530–538.
Breeker, D.O., Sharp, Z.D., McFadden, L.D., 2009. Seasonal bias in the formation and stable isotopic composition of pedogenic carbonate in modern soils from central New Mexico, USA. Geol. Soc. Am. Bull. 121, 630–640.
Burbank, D.W., Meigs, A., Brozovic, N., 1996. Interactions of growing folds and coeval depositional systems. Basin Res. 8, 199–223.
Clark, M.K., Royden, L.H., 2000. Topographic ooze: building the eastern margin of Tibet by lower crustal flow. Geology 28, 703–706.
DeCelles, P.G., Ducea, M.N., Kapp, P., Zandt, G., 2009. Cyclicity in Cordilleran orogenic systems. Nat. Geosci. 2, 251–257.
DeCelles, P.G., Horton, B.K., 2003. Early to middle Tertiary foreland basin development and the history of Andean crustal shortening in Bolivia. Geol. Soc. Am. Bull. 115, 58–77.
Dennis, K.J., Affek, H.P., Passey, B.H., Schrag, D.P., Eiler, J.M., 2011. Defining an absolute reference frame for 'clumped' isotope studies of CO_2. Geochim. Cosmochim. Acta 75, 7117–7131.
Ehlers, T.A., Poulsen, C.J., 2009. Influence of Andean uplift on climate and paleoaltimetry estimates. Earth Planet. Sci. Lett. 281, 238–248.
Eiler, J., 2007. "Clumped-isotope" geochemistry—the study of naturally-occurring, multiply-substituted isotopologues. Earth Planet. Sci. Lett. 262, 309–327.
Eiler, J., 2011. Paleoclimate reconstruction using carbonate clumped isotope thermometry. Quat. Sci. Rev. 30, 3575–3588.
Garzione, C.N., Dettman, D.L., Horton, B.K., 2004. Carbonate oxygen isotope paleoaltimetry: evaluating the effect of diagenesis on paleoelevation estimates for the Tibetan plateau. Palaeogeogr. Palaeoclimatol. Palaeoecol. 212, 119–140.
Garzione, C.N., Hoke, G.D., Libarkin, J.C., Withers, S., MacFadden, B., Eiler, J., Ghosh, P., Mulch, A., 2008. Rise of the Andes. Science 320, 1304–1307.
Garzione, C.N., Molnar, P., Libarkin, J.C., MacFadden, B.J., 2006. Rapid late Miocene rise of the Bolivian Altiplano: evidence for removal of mantle lithosphere. Earth Planet. Sci. Lett. 241, 543–556.
Garzione, C.N., Smith, J.J.-S., Auerbach, D., Rosario, J., Passey, B., Jordan, T., Eiler, J. Diachronous rapid surface cooling of the Bolivian Altiplano: surface uplift or climate change? Geology, in review.
Geobol, 1993. Carta Geologica de Bolivia, Ichoa (Hoja 6142). Servicio Geologico de Bolivia, La Paz.
Ghosh, P., Garzione, C.N., Eiler, J.M., 2006. Rapid uplift of the Altiplano revealed through C-13–O-18 bonds in paleosol carbonates. Science 311, 511–515.
Gillis, R.J., Horton, B.K., Grove, M., 2006. Thermochronology and upper crustal structure of the Cordillera Real: implications for Cenozoic exhumation history of the central Andean Plateau. Tectonics 25, TC6007, http://dx.doi.org/10.1029/2005TC001887.
Gogus, O.H., Pysklywec, R.N., 2008. Near-surface diagnostics of dripping or delaminating lithosphere. J. Geophys. Res. 113, B11404, http://dx.doi.org/10.1029/2007JB005123.
Gonfiantini, R., Roche, M.A., Olivry, J.C., Fontes, J.C., Zuppi, G.M., 2001. The altitude effect on the isotopic composition of tropical rains. Chem. Geol. 181, 147–167.
Gregory-Wodzicki, K.M., 2000. Uplift history of the Central and Northern Andes: a review. Geol. Soc. Am. Bull. 112, 1091–1105.
Hoke, G.D., Garzione, C.N., 2008. Paleosurfaces, paleoelevation, and the mechanisms for the late Miocene topographic development of the Altiplano plateau. Earth Planet. Sci. Lett. 271, 192–201.
Hoke, L., Hilton, D.R., Lamb, S.H., Hammerschmidt, K., Friedrichsen, H., 1994. He-3 evidence for a wide zone of active mantle melting beneath the Central Andes. Earth Planet. Sci. Lett. 128, 341–355.
Horton, B.K., 1998. Sediment accumulation on top of the Andean orogenic wedge: Oligocene to late Miocene basins of the Eastern Cordillera, southern Bolivia. Geol. Soc. Am. Bull. 110, 1174–1192.
Horton, B.K., Hampton, B.A., Waanders, G.L., 2001. Paleogene synorogenic sedimentation in the Altiplano plateau and implications for initial mountain building in the central Andes. Geol. Soc. Am. Bull. 113, 1387–1400.
Huntington, K.W., Eiler, J.M., Affek, H.P., Guo, W., Bonifacie, M., Yeung, L.Y., Thiagarajan, N., Passey, B., Tripati, A., Daëron, M., Came, R., 2009. Methods and limitations of 'clumped' CO_2 isotope ($\Delta 47$) analysis by gas-source isotope ratio mass spectrometry. J. Mass Spectrom. 44, 1318–1329.
Insel, N., Poulsen, C.J., Ehlers, T.A., Sturm, C., 2012. Response of meteoric D18O to surface uplift—implications for Cenozoic Andean Plateau growth. Earth Planet. Sci. Lett. 317–318, 262–272.
Jeffery, M.L., 2012. Impacts of Cenozoic global cooling, surface uplift, and an inland seaway on South American paleoclimate and precipitation D18O. Geol. Soc. Am. Bull. 124, 335–351.
Kay, R.F., MacFadden, B.J., Madden, R.H., Sandeman, H., Anaya, F., 1998. Revised age of the Salla beds, Bolivia, and its bearing on the age of the Deseadan South American Land Mammal "Age". J. Vertebr. Paleontol. 18, 189–199.
Kay, R.W., Kay, S.M., 1993. Delamination and delamination magmatism. Tectonophysics 219, 177–189.
Kim, S.T., O'Neil, J.R., 1997. Equilibrium and nonequilibrium oxygen isotope effects in synthetic carbonates. Geochim. Cosmochim. Acta 61, 3461–3475.
Kley, J., Monaldi, C.R., 1998. Tectonic shortening and crustal thickness in the Central Andes: how good is the correlation? Geology 26, 723–726.
Lamb, S., 2011. Did shortening in thick crust cause rapid Late Cenozoic uplift in the northern Bolivian Andes? J. Geol. Soc. 168, 1079–1092.
Lamb, S., Hoke, L., 1997. Origin of the high plateau in the Central Andes, Bolivia, South America. Tectonics 16, 623–649.
Leier, A.L., McQuarrie, N., Horton, B.K., Gehrels, G.E., 2010. Upper Oligocene conglomerates of the Altiplano, Central Andes: the record of deposition and deformation along the margin of a hinterland basin. J. Sediment. Res. 80, 750–762.
Leier, A.L., Quade, J., DeCelles, P.G., Kapp, P., 2009. Stable isotopic results from paleosol carbonate in south Asia: paleoenvironmental reconstructions and selective alteration. Earth Planet. Sci. Lett. 279, 242–254.
MacFadden, B.J., Campbell, K.E., Cifelli, R.L., Siles, O., Johnson, N.M., Naeser, C.W., Zeitler, P.K., 1985. Magnetic polarity stratigraphy and mammalian fauna of the Deseadan (Late Oligocene Early Miocene) Salla Beds of Northern Bolivia. J. Geol. 93, 223–250.
McQuarrie, N., 2002a. Initial plate geometry, shortening variations, and evolution of the Bolivian orocline. Geology 30, 867–870.
McQuarrie, N., 2002b. The kinematic history of the central Andean fold–thrust belt, Bolivia: implications for building a high plateau. Geol. Soc. Am. Bull. 114, 950–963.
McQuarrie, N., Barnes, J.B., Ehlers, T.A., 2008a. Geometric, kinematic, and erosional history of the central Andean Plateau, Bolivia (15–17 degrees S). Tectonics27, TC3007, http://dx.doi.org/10.1029/2006TC002054.
McQuarrie, N., DeCelles, P., 2001. Geometry and structural evolution of the central Andean backthrust belt, Bolivia. Tectonics 20, 669–692.
McQuarrie, N., Ehlers, T.A., Barnes, J.B., Meade, B., 2008b. Temporal variation in climate and tectonic coupling in the central Andes. Geology 36, 999–1002.

McQuarrie, N., Horton, B.K., Zandt, G., Beck, S., DeCelles, P.G., 2005. Lithospheric evolution of the Andean fold–thrust belt, Bolivia, and the origin of the central Andean plateau. Tectonophysics 399, 15–37.

McRae, L.E., 1990. Paleomagnetic isochrons, unsteadiness, and nonuniformity of sedimentation in Miocene intermontane basin sediments at Salla, Eastern Andean Cordillera, Bolivia. J. Geol. 98, 479–500.

Montgomery, D.R., Brandon, M.T., 2002. Topographic controls on erosion rates in tectonically active mountain ranges. Earth Planet. Sci. Lett. 201, 481–489.

Oncken, O., Hindle, D., Kley, J., Elger, K., Victor, P., Schemmann, K., 2006. Defomration of the Central Andean upper plate system—facts, fiction and constraints for plateau models. In: Oncken, O., Chong, G., Franz, G., Giese, P., Gotze, H.J., Ramos, V., Strecker, M., Wigger, P. (Eds.), The Andes—Active Subduction Orogeny. Springer, New York, pp. 3–27.

Pardo Casas, F., Molnar, P., 1987. Relative motion of the Nazca (Farallon) and South-American plates since Late Cretaceous time. Tectonics 6, 233–248.

Passey, B.H., Henkes, G.A., 2012. Carbonate clumped isotope bond reordering and geospeedometry. Earth Planet. Sci. Lett. 351–352, 223–236.

Passey, B.H., Levin, N.E., Cerling, T.E., Brown, F.H., Eiler, J.M., 2010. High-temperature environments of human evolution in East Africa based on bond ordering in paleosol carbonates. Proc. Natl. Acad. Sci. 107, 11245–11249.

Peters, N.A., Huntington, K., Hoke, G.D., 2013. Hot or not? Impact of seasonally variable soil carbonate formation on paleotermperature and O-isotope records from clumped isotope thermometry. Earth Planet. Sci. Lett. 361, 208–218.

Picard, D., Sempere, T., Plantard, O., 2008. Direction and timing of uplift propogation in the Peruvian Andes deduced from molecular phylogenetics of highland biotaxa. Earth Planet. Sci. Lett. 271, 326–336.

Poage, M.A., Chamberlain, C.P., 2001. Empirical relationships between elevation and the stable isotope composition of precipitation and surface waters: considerations for studies of paleoelevation change. Am. J. Sci. 301, 1–15.

Poulsen, C.J., Jeffery, M.L., 2011. Climate change imprinting on stable isotopic compositions of high-elevation meteoric water cloaks past surface elevations of major orogens. Geology 39, 595–598.

Quade, J., Eiler, J., Daeron, M., Achyuthan, H., 2013. The clumped isotope geothermometer in soil and paleosol carbonate. Geochim. Cosmochim. Acta 105, 92–107.

Quade, J., Garzione, C., Eiler, J., 2007. Paleoelevation reconstruction using pedogenic carbonates. Rev. Mineral. Geochem. 66, 53–87.

Roeder, D., 1988. Andean-age structure of Eastern Cordillera (Province of La-Paz, Bolivia). Tectonics 7, 23–39.

Rowley, D.B., Garzione, C.N., 2007. Stable isotope-based paleoaltimetry. Annu. Rev. Earth Planet. Sci. 35, 463–508.

Saleeby, J., Foster, Z., 2004. Topographic response to mantle lithosphere removal in the southern Sierra Nevada region, California. Geology 32, 245–248.

Sempere, T., Butler, R.F., Richards, D.R., Marshall, L.G., Sharp, W., Swisher, C.C., 1997. Stratigraphy and chronology of upper Cretaceous lower Paleogene strata in Bolivia and northwest Argentina. Geol. Soc. Am. Bull. 109, 709–727.

Sempere, T., Herail, G., Oller, J., Bonhomme, M.G., 1990. Late Oligocene Early Miocene major tectonic crisis and related basins in Bolivia. Geology 18, 946–949.

Sobel, E.R., Hilley, G.E., Strecker, M.R., 2003. Formation of internally drained contractional basins by aridity-limited bedrock incision. J. Geophys. Res.—Solid Earth, 2334, http://dx.doi.org/10.1029/2002JB001883.

Sobolev, S.V., Babeyko, A.Y., 2005. What drives orogeny in the Andes? Geology 33, 617–620.

⟨http://www.climate-zone.com⟩, 2012. Bolivia, Average Monthly Climate Indicators Based on 8 years of Historical Weather Readings.

Zachos, J., Pagani, M., Sloan, L., Thomas, E., Billups, K., 2001. Trends, rhythms, and aberrations in global climate 65 Ma to present. Science 292, 686–693.